STRUCTURAL PERFORMANCE OF AN ELECTRIC ROAD SYSTEM USING ACCELERATED LOAD TESTS

B. KALMAN
Swedish National Road and Transport Research Institute (VTI)
Ph.D. in Physical Chemistry, Umeå University.
Research Director Road and Railway Engineering

L. NORDIN
Swedish National Road and Transport Research Institute (VTI)
Ph.D. in Science, Physical Geography
Research Director Infrastructure Maintenance

Abstract

An Electric Road System (ERS) is one option to enhance the operating range of battery electric vehicles without stops for charging. A comprehensive study of the performance of a road structure with an embedded ERS has been carried out with a Heavy Vehicle Simulator (HVS). The rail for conductive dynamic charging while in motion is placed between the wheel paths in the road. In the first phase of the study the ERS system was subjected to overpasses of a truck tire loaded to 6 kN in dry and wet conditions until the beginning of failure. The overpass test was performed to check how many times a truck could make a lane change, crossing the ERS. In the second phase the performance of the road structure with an ERS installed was evaluated with the HVS. The road structure was a typical Swedish high-capacity road structure where the bound asphalt layer thickness was 210 mm thick placed on 500 mm unbound layers of crushed rock. Strain gauges and pressure cells were placed in asphalt layers close to the ERS and in a reference area. The responses from the gauges were compared and analyzed considering the typical lateral wandering of heavy vehicles on Swedish motorways. The conclusion is that the structural performance of the road with an ERS installed, and the reference road are similar.

Keywords: Electric Road System, Heavy Vehicle Simulator, Accelerated Load Test, Dynamic Charging

1. Background

Battery powered electrical heavy vehicles are expected to be introduced in large scale to reduce pollution and CO_2 emissions. The weight of batteries decreases the payload of trucks. To reduce the size of the batteries or to increase the operating range without having to stop and recharge the batteries, solutions to recharge the batteries while driving are becoming an interesting solution. There are different technologies available to power vehicles while driving and one option is to use a conductive rail installed within the road.

An electrical road, where new components are introduced in the road structure could change how the asphalt layers respond to loads. Introducing non-asphalt concrete materials in the structure changes the load bearing capacity in vicinity of the new components and could furthermore make the structure more prone to delamination in the contact zone between the asphalt and the new components.

Roads made with thick bituminous bound layers usually fail structurally in the long run due to fatigue cracking. Before a road eventually reaches its structural limit, the surface course is replaced several times. The traffic will create ruts in the wheel paths either due to plastic deformation caused by heavy traffic or in the countries where studded tires are used, due to road wear caused by studded tires. Road surface unevenness is increasing as the road gets older. Resurfacing operations will restore the surface evenness. Nevertheless, the structural degradation will continue since it often starts as fatigue crack formations at the bottom of the bituminous layers due to repeated strains created by heavy traffic.

2. Objective

The purpose of this study was to measure how a typical Swedish asphalt construction for the high-volume traffic road network is affected by charging infrastructure being installed in milling boxes on the surface of the roadway between the wheel tracks and to estimate how the installation will affect the service life of the road construction. Truck tires running over the charging segments simulating lane changes as also studied with the accelerated load facility.

3. Method

Two sets of tests were performed. Firstly, an observational study was performed where different designs of the charging rails were installed in milling boxes. Accelerated loading tests were performed with a Heavy Vehicle Simulator (HVS). The charging rails were installed at an angle vs the loading wheel in the HVS. The test simulated a truck tire running across the rail during a change of lanes. The truck tire load was 6 kN, correspond to an axel load of 12 kN, and the HVS was running at 12 km/h. The second phase of the trial consisted of measurements of strain and pressure at strategic positions around the charging rail.

3.1 Road structure

The road structure used in the experiments was that of a typical Swedish high-volume road. Sweden builds relatively thin asphalt pavement structures on a base of crushed rock material. The structure was built in a test hall 5 meters wide and 15 meters long. The test hall is three meters deep. The bottom and sidewalls are made of concrete. The structure used for the experiment was made of the following layers from the deepest layers to the top:

- Terrace: 2300 mm silty sand

- Sub-base: 420 mm 0/90 crushed rock
- Road base: 80 mm 0/32 crushed rock
- Bound base course: 110 mm AC22 (AG22; penetration bitumen 100/150; 4.7% by weight binder content)
- Binder course: 60 mm BC22 (ABb22; penetration bitumen 50/70; 5.4% by weight binder content)
- Surface course: 40 mm SMA16 (ABS16; penetration bitumen 70/100; 6.2% by weight binder content; 0.4% cellulosa fiber)

All bound layers contained 0.3% by weight of Wetfix BE adhesion promotor. Air voids in Marshall samples were 4.0%; 3.0% and 2.6% for the base course, binder course and the surface course, respectively.

After laying the surface course the construction was preloaded using the HVS. A total of 20,000 passes with a 50 kN load and with a ring pressure of 700 kPa were performed. The rolling truck tire load was evenly distributed over the entire loaded surface, which is 8 by 1.3 meters, by moving the wheel after every 20 crossings in 5 cm increments from -35 cm to +35 cm relative to the centerline under the HVS.

3.2 Installation of conductive rail

60 mm deep and 400 mm wide boxes were milled out from the surface to house the conductive rails from Elonroad. A rail installed in a road is shown in. The rails were installed by having them attached to bars which rested on the undisturbed surface. The void beneath the rail and up to 20 mm from the undisturbed surface was filled with InfraRoad Undergjutningsmassa (undercasting mastic). After cooling and removing the bars, the last 20 mm of the void was filled with InfraRail Railjoint. The two products were provided by InfraCare AB.

Figure 1 Conductive rail installed on a road

3.3 Sensors

Strain gauges and pressure cells were installed in the second phase of the trials. Seventeen strain gauges of model PAST-2 from Dynatest A/S were installed, mostly at the bottom of the asphalt concrete construction. However, two were installed in the surface close to the short ends of the rails and one was placed in the milled box beneath the conductive rail. Each strain gauge is 102

mm long and is attached to two 77 mm bars at the end. The measuring range was up to 1500 µstrain.

Two pressure cells, SOPT 68b from Dynatest, were placed between the sub-base and the road base, 80 mm below the asphalt concrete. These are 65 mm in diameter, 15 mm thick and can record pressure between 100 to 800 kPa.

The layout of the rail and sensors are schematically shown in Figure 2. In the figure the lateral end points of the twin truck tire are indicated. The sensors are placed in four groups designated as Group T1, L1, L2 and T2, respectively. Individual strain gauges are designated as A1 to A17.

3.4 Response measurements

Response measurements, i.e. the signal from the strain and pressure transducers respectively, were performed as the load wheel rolled along each position in 50 mm increments from -350 mm to +350 mm relative to the center line. At each response measurement, for each load case, 20 passes were made with the load wheel and the signal from the respective sensor was collected for the last 4 passes. The experiments were performed at 8 °C, 0 °C and 30 °C. The different load cases are summarized in Table 1.

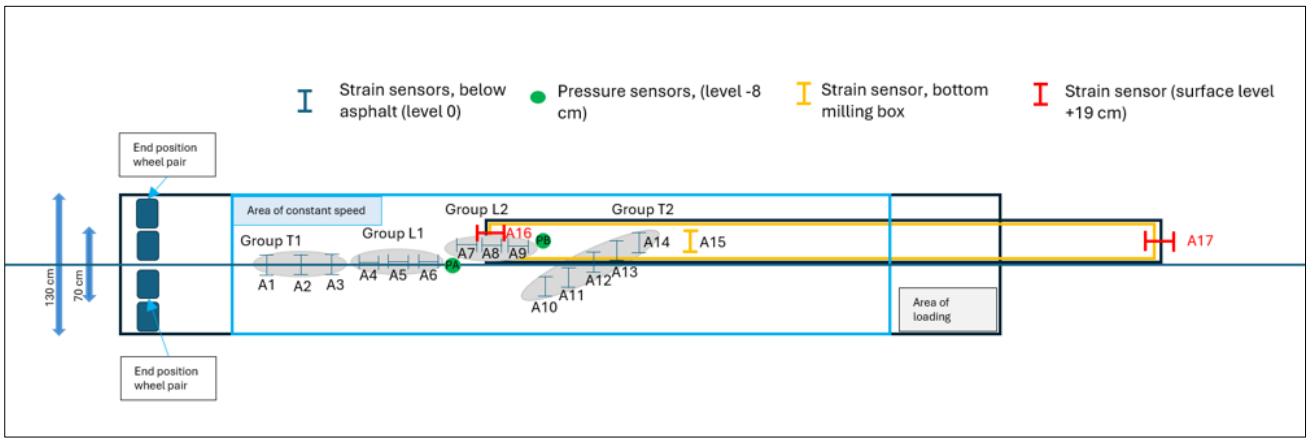

Figure 2 Layout of sensors and conductive rail for response measurement

Table 1 Load cases

Tire pressure (kPa)	Load (kN)	Designation
700	50	P700-50
800	30	P800-30
800	40	P800-40
800	50	P800-50
800	60	P800-60
800	80	P800-80
900	50	P900-50

The sensor group T1 records the transverse strain at the bottom of the asphalt layer in an area unaffected by the electric road rail. The L1 group records the longitudinal strain at the bottom of the asphalt layer in an area unaffected by the electric road rail. Although group L1 and T1 are not placed in a position relative to the conductive rail that corresponds to the position of the wheel track on a road in the field, the response measurements in this undisturbed position can be used to represent the strains in the wheel path on an actual road. The L2 and T2 groups register longitudinal and transverse strains at the bottom of the asphalt layer in positions around the electric road rail.

4. Results and discussion

4.1 Accelerated overtaking test

Two different designs of the charging rails installed in milling boxes were compared. The boxes and rails were installed at an angle vs the loading wheel in the HVS to simulate a truck tire running over the rail during a change of lanes. In total 230 000 overpasses were made with a load of 6 kN. The test was segmented into six test phases as detailed in Table 2.

Table 2 Accelerated overtaking test phases

Test phase #	Number of passes	Conditions
1	30 000	Dry, ambient outdoor October temperatures
2	20 000	Wet, ambient outdoor November temperatures
3	45 000	Dry, subzero temperatures between -2 −-5°C
4	5 000	Wet, 10 °C
5	65 000	Dry, temperature drifting slowly back and forth between zero and -7 °C
6	65 000	Wet, zero degrees
Total	230 000	

For the simpler of the two designs tested an adhesion failure occurred between one side of the rail and the rail joint in the third test phase but the rail still stayed in place for the whole duration of the test. The adhesion of the more advanced rail design did not show any sign of deterioration throughout the test.

We do not have data on how often trucks change lanes although our perception is that trucks are engaged in changing lanes less than 1 percent of the time. If so, we would expect that the more advanced design of the rails will sustain more than 20 million heavy vehicle passes.

4.2 Response measurements

Roads made with thick bituminous bound layers are prone to fatigue cracking. The fatigue cracking starts in areas where there is strain in the structure. Fatigue initiation and propagation are strain dependent and naturally stochastic processes. The strain is usually highest at the bottom of the asphalt layers and the strain, ε_t, is proportional to the axle load. The number of load cycles until failure, N_f, depends on the strain level and on the structural and material parameters, k_1 and k_2.

$$N_f = k_1 \left(\frac{1}{\varepsilon_t}\right)^{k_2} \quad (1)$$

The degradation rate usually increases with the strain level raised to the power of four, or in the range 3–4 (Said, 1997; Huang, 2004) i.e. $k_2 \sim 4$. This is usually denoted the 4th power law which has been disputed but is still universally used in structural pavement analysis.

For the purpose to compare the effect of strains in different locations it is convenient to define the damage ratio, *D*.

$$D = \left(\frac{\varepsilon_{t2}}{\varepsilon_{ref}}\right)^4 \quad (2)$$

Where ε_{ref} is the strain in the reference area. Since the strain typically is highest at the bottom of the asphalt layers and most load repetitions are created by the traffic in the center of the wheel track, it is convenient to choose the strain there as the reference strain.

Typical transversal and longitudinal strains from group T1 and group L1 are shown in Figure 3.

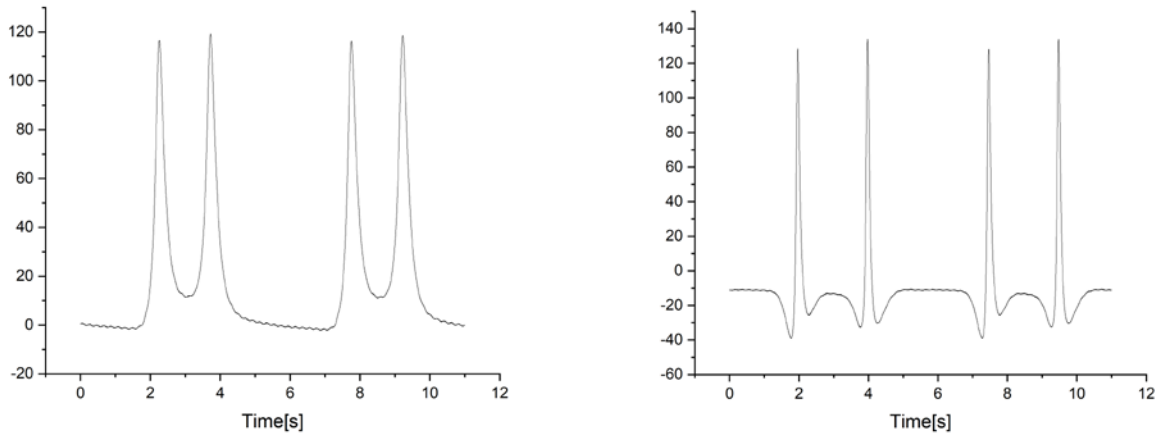

Figure 3 Transversal (left) and longitudinal (right) strain (µstrain) at the bottom of the asphalt concrete layers in group T1 and L1. Tire pressure 800 kPa, load 50 kN, temperature 8 °C

In Figure 4 the average value of the maximum strains for groups T1 and L1 for different load cases at 0 °C is shown. Figure 4 show that the strains in the underside of asphalt are almost linearly dependent on the load. The maximum longitudinal strains are slightly higher than the transverse strains.

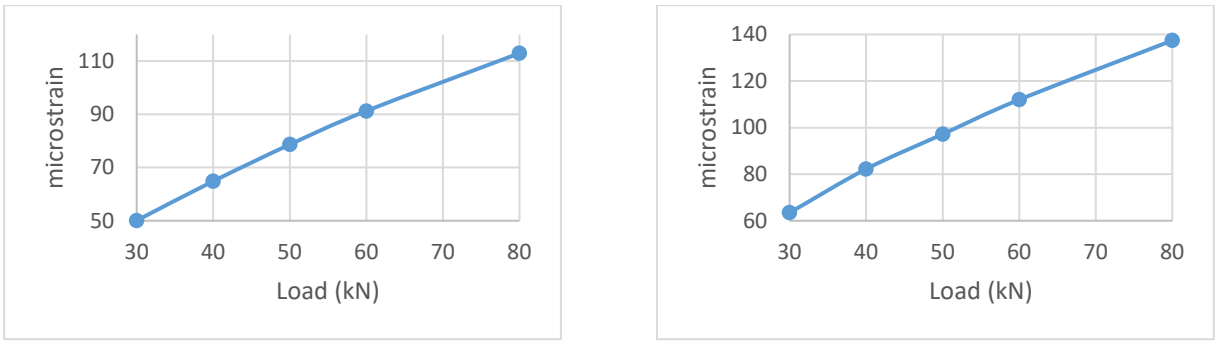

Figure 4 Average maximum transversal (left) and longitudinal (right) strains in group T1 and L1 at 0°C. Tire pressure 800 kPa

The maximum longitudinal strains at the bottom of the asphalt layers at the short end of the conductive rail were measured with longitudinal strain gauges in group L2. The data is shown in Figure 5.

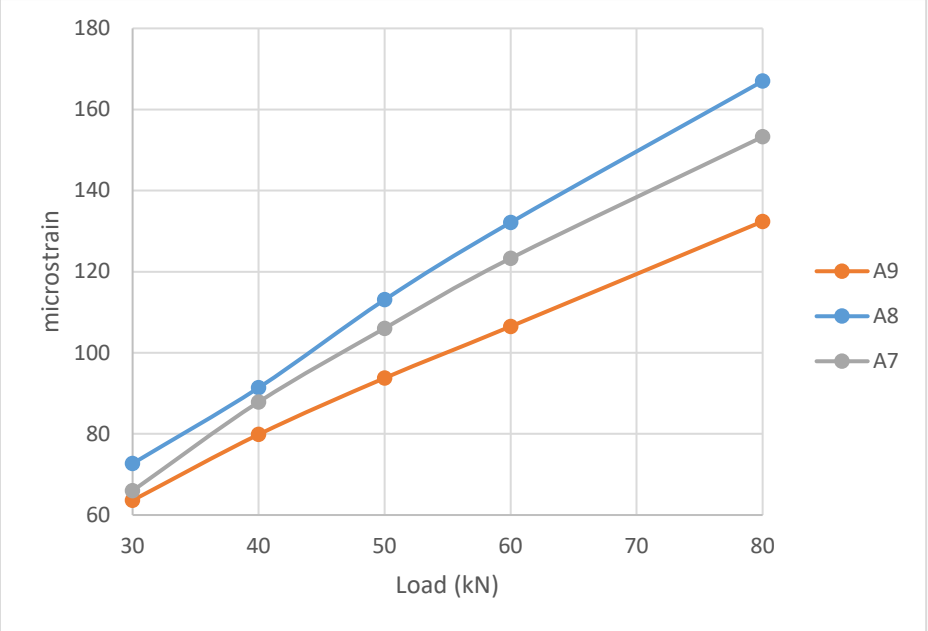

Figure 5 Maximum longitudinal strain in group L2 at 0°C. Tire pressure 800 kPa

Of the three strain sensors, the highest strain was obtained for the sensor, A8, which was placed directly under the transition between asphalt and the conductive rail, see Figure 2. The sensor, A9, which is located under the short end of the rail, has a lower strain level than A7, which is in close connection to the rail but not under it.

The damage ratio for sensor A8 is calculated for different load cases according to equation 2 with the longitudinal maximum strains in wheel tracks, see Figure 4, as reference levels. The load cases are presented in Table 1. The damage ratios are presented in Figure 6. The damage ratio varies between 1.5 and 2.2.

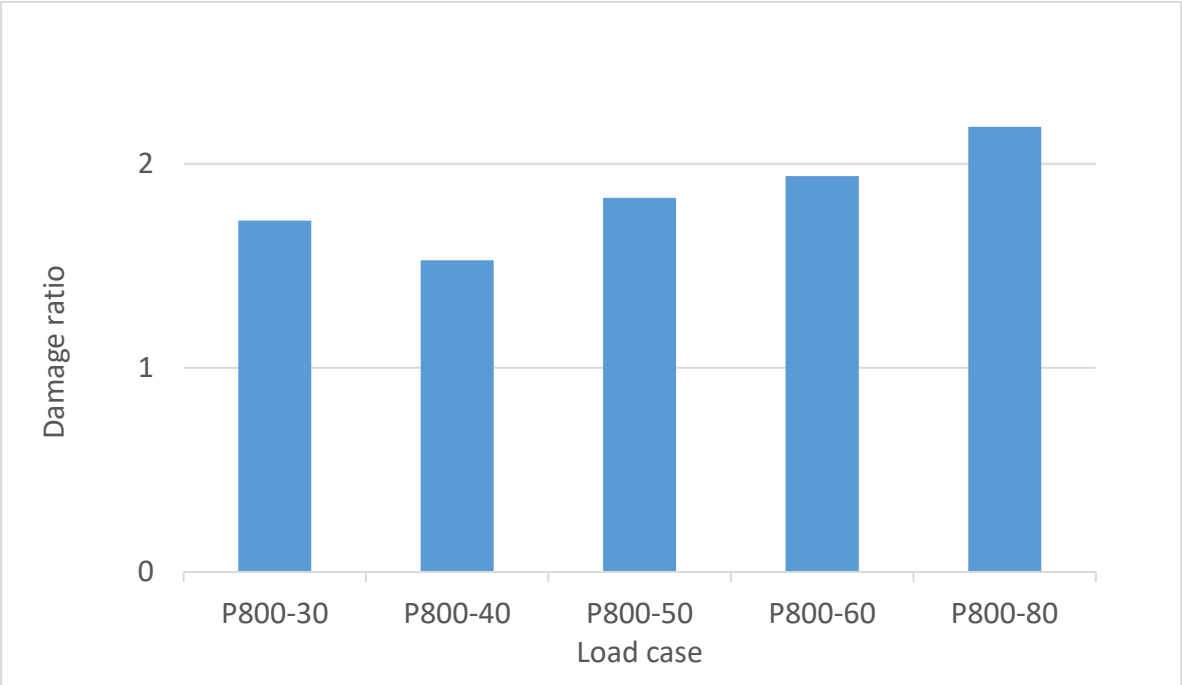

Figure 6 Damage ratio for the asphalt concrete under the short end of a conductive rail compared to the wheel track at 0°C for different load cases.

To determine where the maximum strains occur in the underside of the asphalt on the side of the conductive rail, the strain sensors in group T2 were placed offset in relation to each other according to Figure 2. The response from these sensors is presented in Figure 7.

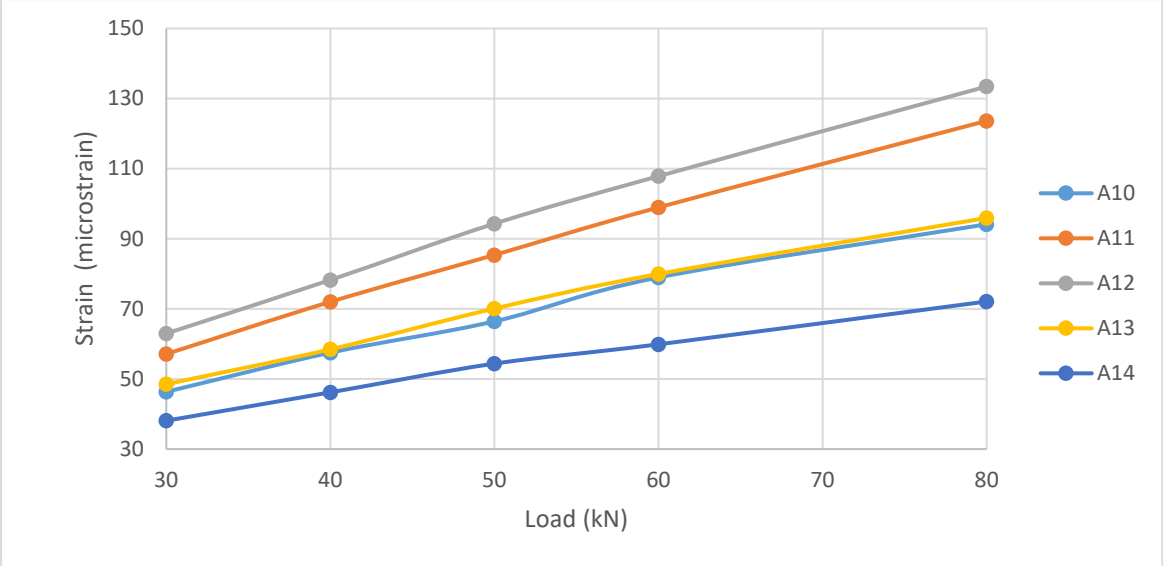

Figure 7 Maximum transversal strain in group T2 at 0°C. Tire pressure 800 kPa

The lowest strain levels were obtained for the sensor A14 which is located under the rail and the highest strain level was obtained for A12 whose location just spans the edge of the milling box and the conductive rail, see Figure 2.

The damage ratio for the asphalt around strain gauge A12 with the highest strain levels is calculated according to equation 2 versus the transverse maximum strains in wheel tracks, see Figure 8.

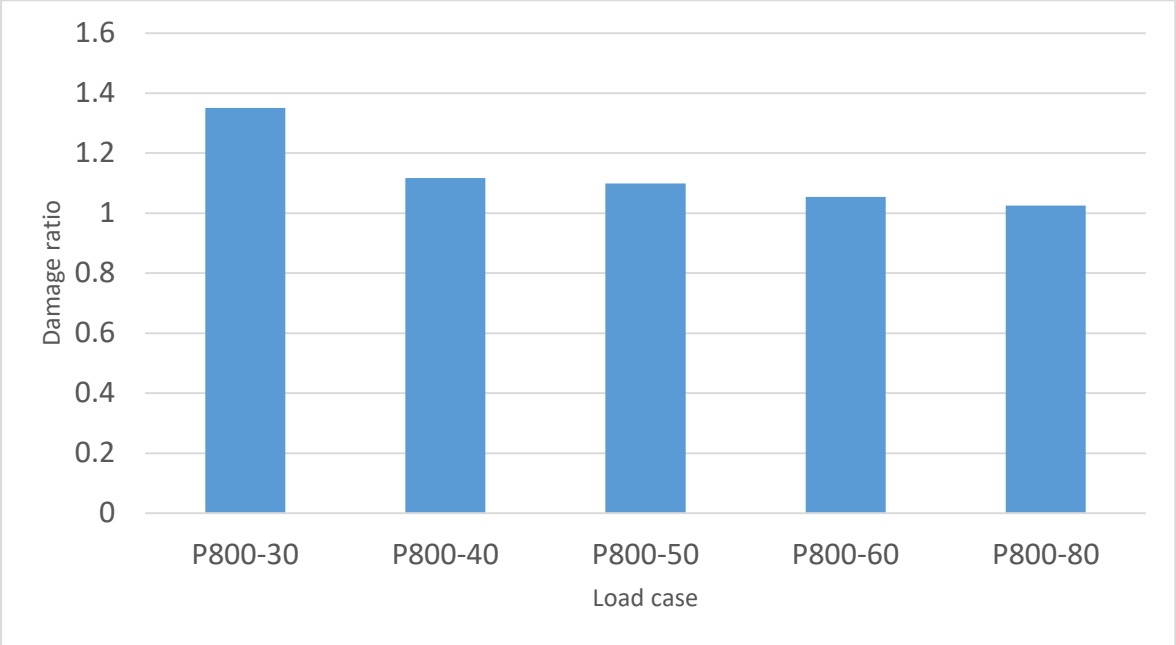

Figure 8 Damage ratio for the asphalt concrete under the long edge of a conductive rail compared to the wheel track at 0°C for different load cases.

The damage ratio of asphalt at the transition between the road surface and the conductive rail varies between 1.02 and 1.35.

Lateral Wandering and Probability Damage Ratio

The lateral wander of wheel loads on roads depends on the lane width, vehicle types, the existence of road shoulders, and traffic speed (Blab and Litzka 1995, Timm and Priest 2005, McGarvey 2016). The lateral wander of heavy trucks can be described with a normal distribution (McGarvey 2016). The standard deviation of the normal distribution depends on the type of road. For Swedish motorways the standard deviation for lateral wandering for heavy trucks is approximately 240 mm (220-250 mm). Figure 9 shows the lateral position of heavy vehicles with a front axle track width of 2.1 meters. The vehicles' positions are relative to the left-hand side lane marking. The conductive rail box is drawn to scale between the wheel tracks.

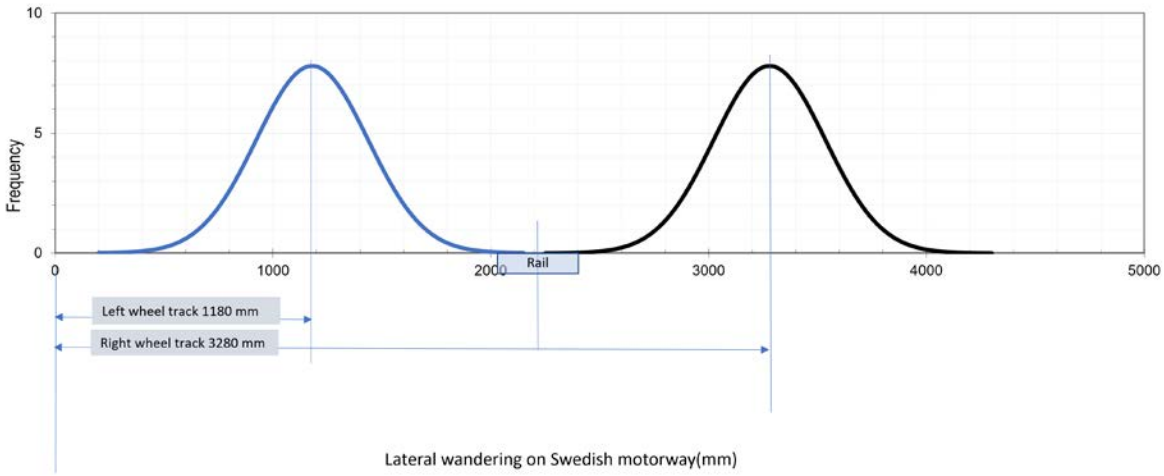

Figure 9 Wheel track distribution of heavy trucks on Swedish motorway

It is obvious that the road areas hosting the conductive rail is less trafficked than the area of the center of the wheel track. It is therefore necessary to consider the difference in loading frequency in the wheel track compared to other parts of the road when comparing the damage ratio, D, for those parts. The probabilistic damage ratio, D_P , is defined as

$$D_P = D\frac{f}{f_{ref}} \tag{3}$$

Where f and f_{ref} are the traffic frequency in the area of interest and in the center of the wheel path, respectively. If the probabilistic damage ratio is less than one, it shows that it is more likely that fatigue cracking is initiated in the wheel path than in the area under study. And vice versa if the probabilistic damage ratio is greater than one it is more likely that cracks will begin in the area under study before they will be initiated in the wheel path.

The edge of the electric rail is trafficked less frequently than the area under the wheel track. To assess the probability that structural damage to the asphalt occurs because of the weakening of the construction at the transition between the asphalt surface and the electric rail, the damage ratio needs to be corrected for the lateral distribution of the traffic according to equation 3. The distance between the center of the wheel track and the edge to the electric rail is approximately 900 mm. The ratio of the loading frequencies f and f_{ref} is 0.00207 when the standard deviation of the lateral position distribution is 256 mm, as measured on Swedish motorways (McGarvey 2016). The probabilistic damage ratio for fatigue cracking in the asphalt at the transition between the asphalt and rail D_P is presented in Figure 10.

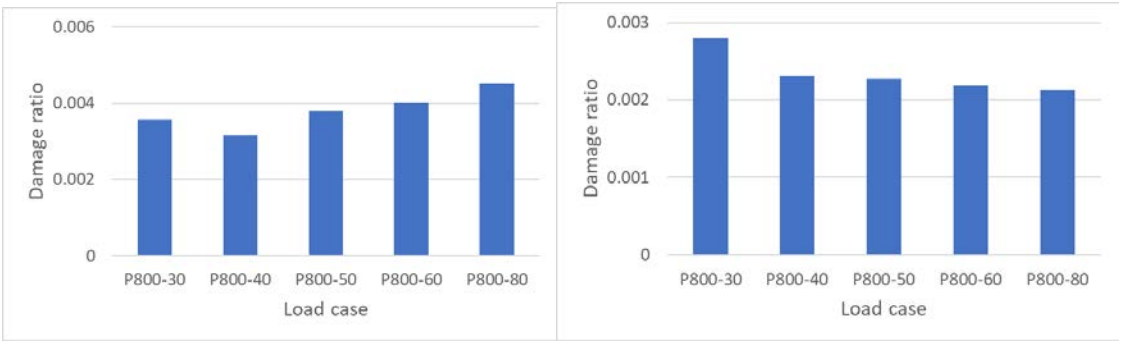

Figure 10 Probabilistic damage ratios for the asphalt concrete under the short end (left) and the long edge (right) versus the wheel path.

The probabilistic damage ratio varies between 0.0021 and 0.0045 with respect to fatigue cracks at the bottom of the asphalt concrete below the edges of the conductive rail compared to the asphalt concrete in wheel tracks.

5. Conclusions

Tensile strains occur in the lower half of the asphalt construction under the wheel and on the upper part of the construction around and at some distance from the wheel. In other parts of the asphalt, such as the upper part of the asphalt construction under the wheel, compression strains occur instead. Normally, the tensile strains are highest at the lower edge of the asphalt construction. The probability is therefore highest that fatigue cracks start at the lower edge of the asphalt, but they can also appear in other parts if the strains are large and frequent. Once a crack forms, it will continue to grow under load, eventually reaching through the entire structure. In this study, we have investigated where tensile strains occur in a typical Swedish motorway construction when a conductive electric rail is mounted in a milled box between the wheel tracks and compared these strains with the tensile strains that occur in the wheel track. The tensile strains at the bottom of the asphalt layers were slightly higher under the edges of the conductive rail than in the wheel track when the same load was applied to the two areas. The strains were between 0 and 20% higher under the edges of the conductive rail compared to the strains in wheel tracks. The significance of this increase in strain levels for the structural life of the road is negligible because the lateral distribution of heavy traffic on highways is limited. Field studies have shown that the standard deviation for the lateral position distribution is approximately 250 mm on Swedish motorways. If this is considered, the probability of cracks being initiated under the conductive rail is less than half a percent compared to the area under the wheel track. The structural life of a highway will, based on this, not be affected by the installation of a conductive rail between wheel tracks.

An accelerated load test to simulate truck tires passing over the conductive rail was also performed. The test was stopped after 230000 passes with no apparent failures for a rail designed to be attached to the asphalt concrete.

6. References

- Blab, R. & Litzka, J. (1995) “Measurements of the lateral distribution of heavy vehicles and its effects on the design of road pavements.” Proceedings of the International Symposium on Heavy Vehicle Weights and Dimensions, Road Transport Technology, 389–395.
- Huang, Y. H. (2004). Pavement analysis and design. USA: Pearson Prentice Hall.
- McGarvey, T. (2016). “Vehicle lateral position depending on road type and lane width.” VTI rapport 892A
- Said, S. (1997). “Variability in roadbase layer properties conducting indirect tensile test.” Proceedings of the 8th international conference on asphalt pavements, Seattle, Washington, pp. 977-986.
- Timm, D. & Priest, A. (2005). “Wheel Wander at the NCAT Test Track.” NCAT Report 05-02